IL-21 is pivotal in determining age-dependent effectiveness of immune responses in a mouse model of human hepatitis B

Jean Publicover,[1,2] Amanda Goodsell,[1,2] Stephen Nishimura,[3] Silvia Vilarinho,[1,2] Zhi-en Wang,[1] Lia Avanesyan,[4,5] Rosanne Spolski,[6] Warren J. Leonard,[6] Stewart Cooper,[2,4,5] and Jody L. Baron[1,2]

[1]Department of Medicine, [2]UCSF Liver Center, and [3]Department of Pathology, UCSF, San Francisco, California, USA. [4]Liver Immunology Laboratory, and [5]Division of Hepatology and Center for Liver Disease, California Pacific Medical Center and Research Institute, San Francisco, California, USA. [6]Laboratory of Molecular Immunology, National Heart, Lung, and Blood Institute, NIH, Bethesda, Maryland, USA.

HBV is a noncytopathic hepadnavirus and major human pathogen that causes immune-mediated acute and chronic hepatitis. The immune response to HBV antigens is age dependent: viral clearance occurs in most adults, while neonates and children usually develop chronic infection and liver disease. Here, we characterize an animal model for HBV infection that recapitulates the key differences in viral clearance between early life and adulthood and find that IL-21 may be part of an effective primary hepatic immune response to HBV. In our model, adult mice showed higher HBV-dependent IL-21 production in liver, compared with that of young mice. Conversely, absence of the IL-21 receptor in adult mice resulted in antigen persistence akin to that of young mice. In humans, levels of IL-21 transcripts were greatly increased in blood samples from acutely infected adults who clear the virus. These observations suggest a different model for the dichotomous, age-dependent outcome of HBV infection in humans, in which decreased IL-21 production in younger patients may hinder generation of crucial $CD8^+$ T and B cell responses. These findings carry implications for therapeutic augmentation of immune responses to HBV and potentially other persistent liver viruses.

Introduction

HBV chronically infects approximately 400 million people and results in more than 0.6 million deaths annually by causing liver failure and liver cancer (1). The chance of clearing HBV infection is age dependent. Ninety-five percent of adult-acquired infections lead to spontaneous clearance, whereas more than 90% of exposed neonates and approximately 30% of children aged 1–5 years will develop chronic infection (2–4). Individuals infected during infancy represent the group that harbors the majority of the global reservoir of hepatitis B and therefore exert the greatest health-care impact. A strong, diverse, adaptive immune response is considered essential for HBV clearance, but what causes an individual to generate a favorable response is largely unknown (5). The current paradigm posits that "immune system immaturity" and "neonatal tolerance" to HBV underpins the greatly increased viral persistence in the young (6–8), but this has not been mechanistically explained or definitively validated. Thus, a fundamental question remains: why is the immune response and disease outcome in HBV infection different depending on the age of the individual at the time of infection? The answers to this question might identify interventions that could promote protective immunity in hosts destined to become chronically infected, which would represent a major therapeutic advance.

Studying the early events in immune activation that determine HBV clearance or persistence is not feasible in young infants and difficult in adult humans. Aside from the intrinsic limitations of tissue acquisition in children, at-risk babies in developed countries receive immune globulin and vaccination to prevent infection. Elsewhere, most new infections are asymptomatic and do not attract medical attention. In adult clinical settings, in which the infrastructure exists to study hepatitis B, patients have generally been infected for decades. Although a few cases of acute adult HBV infection can be studied, these provide sparse opportunity to study persistence, because 90%–95% of adults will clear the virus. Thus, to understand the immune events that underpin HBV clearance or persistence, experimental models of the human disease are vital. Over the past 10 years we have therefore developed a mouse model of primary HBV infection that has allowed us to study the age-dependent differences in immune responses to HBV infection that correlate with viral clearance and viral persistence.

Because HBV cannot infect mice, our laboratory uses transgenic and gene-deficient mouse models that mimic important aspects of primary HBV infection (9, 10). We use 2 lines of HBV-transgenic C57BL/6 mice: HBV-envelope (HBVEnv) mice, which contain the entire HBV envelope-coding region under the transcriptional control of the mouse albumin promoter (11), and HBV-replication (HBVRpl) mice, which contain a terminally redundant HBV DNA construct that allows viral replication and the release of infectious virions (12). The T and B cell adaptive immune system of these HBV-transgenic mice (which are tolerant to HBV antigens) is ablated by crossing them with mice genetically deficient in the recombinase, RAG-1 (*Rag1*$^{-/-}$), which is required to generate mature B and T cells (13). Thus, mice are generated that express viral antigen or intact virus in the liver in the absence of an adaptive immune system. Adoptive transfer of 10^8 HBV-naive, syngeneic splenocytes from wild-type C57BL/6 mice or genetically modified mice reconstitutes the immune system, mimics the point of primary infection, and allows us to test the importance of cellular and soluble mediators in HBV pathogenesis (9).

This model of HBV infection mimics specific and important aspects of primary HBV infection that are otherwise impossible

Conflict of interest: Warren J. Leonard and Rosanne Spolski are inventors on patents and patent applications related to IL-21.

Citation for this article: *J Clin Invest.* 2011;121(3):1154–1162. doi:10.1172/JCI44198.

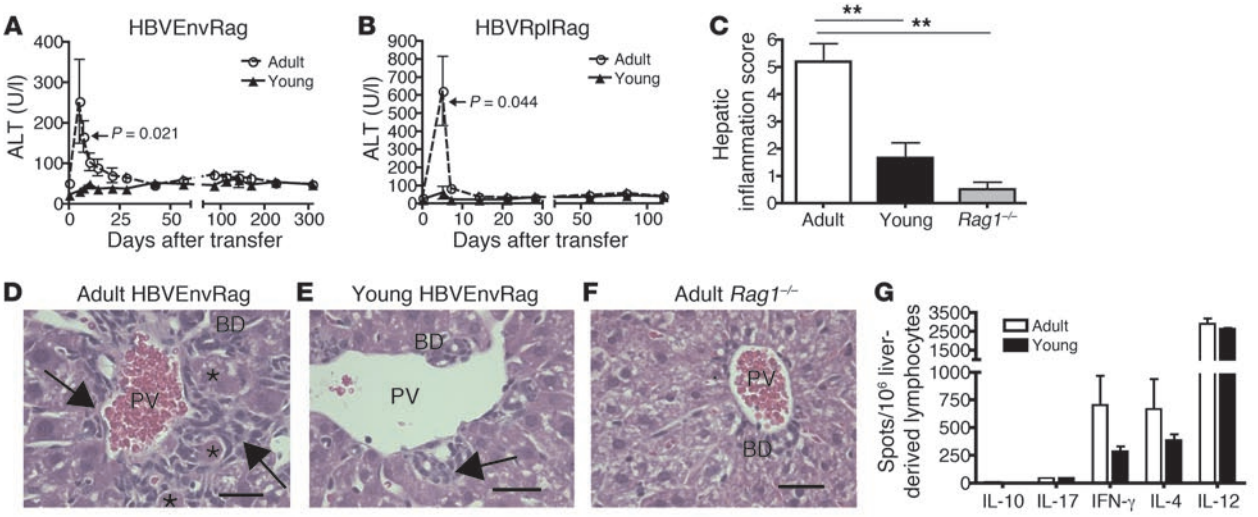

Figure 1

Transfer of adult splenocytes into young and adult HBVtgRag mice results in a difference in disease outcome. Depiction of plasma ALT in young and adult (**A**) HBVEnvRag or (**B**) HBVRplRag mice after adoptive transfer of adult wild-type C57BL/6 mouse splenocytes. Error bars show mean ± SEM. Data are representative of at least 3 separate experiments where $N \geq 5$ mice. Sections from formalin-fixed, paraffin-embedded liver tissue were taken 8 days after adoptive transfer of adult, syngeneic splenocytes and stained for H&E. (**C**) Composite score of necrosis, portal inflammation, and intraparenchymal inflammation as read by an unbiased pathologist. Error bars depict mean ± SEM; $N \geq 5$ mice. Statistical significance was determined using the ANOVA with Tukey's multiple comparison test. $^{**}P < 0.01$. Representative liver H&E stains from (**D**) adult HBVEnvRag, (**E**) young HBVEnvRag, and (**F**) adult HBVtg-negative *Rag1*$^{-/-}$ mice. Arrows point to portal tract inflammation adjacent to the portal vein (PV) and bile duct (BD). Asterisks indicate necrotic hepatocytes. Scale bar: 30 mm. Statistical significance was determined using the unpaired 2-tailed *t* test. (**G**) IL-10, IL-17, IFN-γ, IL-4, and IL-12 cytokine levels were determined by ELISpot assay on liver-derived lymphocytes from adult or young HBVEnvRag mice 8 days after transfer of adult syngeneic splenocytes. Samples were pooled from $n = 4$ mice; error bars represent mean ± SEM from at least 3 separate wells.

to study in humans, including aspects that previous models have been unable to address. Importantly, the naive immune system is primed to virus or antigen expression that originates in the liver and is not biased by prior immunization, prior immune selection during development, or selection for particular immune effector subpopulations. Additionally, the recipient HBV transgenic *Rag1*$^{-/-}$ (HBVtgRag) mice do not have an adaptive immune system that has been rendered tolerant to the virus by virtue of the fact that it has "seen" HBV during immune development. Thus, in this model, virus or viral antigens produced in the liver are engaged by an immune system that is naive to the virus.

We have used this experimental system to probe age-dependent immune responses to HBV. Our adoptive transfer model provides an opportunity to separately dissect the roles of the ages of the immune effector cells and of the immune-priming environment in the development of the HBV-specific immune response and disease outcome. Using this model, we have been able to elucidate potential mechanisms by which the immaturity of the immune-priming environment of effector lymphocytes in newborns and young children contributes substantially to the immune response that leads to HBV persistence and chronic hepatitis.

Results

Different disease outcomes occur in young and adult HBVtgRag mice following adoptive transfer of adult splenocytes. Adoptive transfer of splenocytes from adult (8- to 10-week-old) wild-type mice into adult (8- to 10-week-old) *Rag1*$^{-/-}$ C57BL/6 HBVEnv mice (HBVEnvRag mice) or *Rag1*$^{-/-}$ C57BL/6 HBVRpl mice (HBVRplRag mice) revealed a robust, HBV-dependent inflammatory response and liver injury after adoptive transfer. The mice developed an acute hepatitis, beginning 4–5 days after adoptive transfer, as evidenced by a rise in plasma alanine transaminase (ALT), a measure of hepatic necrosis (Figure 1, A and B). Histological analysis of H&E-stained liver sections from these mice revealed significant HBV-dependent portal and intraparenchymal inflammation as well as hepatic necrosis (Figure 1, C, D, and F).

To assess the contribution of the age of the resident immune-priming environment in the HBVEnvRag or HBVRplRag mice to the immune response to HBV, we adoptively transferred splenocytes from adult (8- to 10-week-old) wild-type mice into young (3- to 4-week-old) HBVEnvRag or HBVRplRag mice. This experiment revealed a strikingly different HBV-dependent inflammatory response. The young transgenic mice that received adult splenocytes never developed ALT elevation and exhibited only minimal HBV-dependent hepatic inflammation, without evidence of hepatic necrosis (Figure 1, A–C, E, and F). No ALT elevation or hepatic inflammation was observed in *Rag1*$^{-/-}$ mice after adoptive transfer (Figure 1F; data not shown). A composite hepatic inflammation score that grades portal inflammation, intraparenchymal inflammation, and necrosis revealed that the adult HBVEnvRag mice had significantly increased hepatic inflammation as compared with that of the young HBVEnvRag mice 8 days after adoptive transfer of splenocytes (Figure 1C). Both the young and adult HBVEnvRag mice had increased hepatic inflammation scores as compared with those of *Rag1*$^{-/-}$ mice (Figure 1C).

ELISpot analysis of liver lymphoid cells at the peak of hepatitis in the adult mice (8 days after adoptive splenocyte transfer) revealed

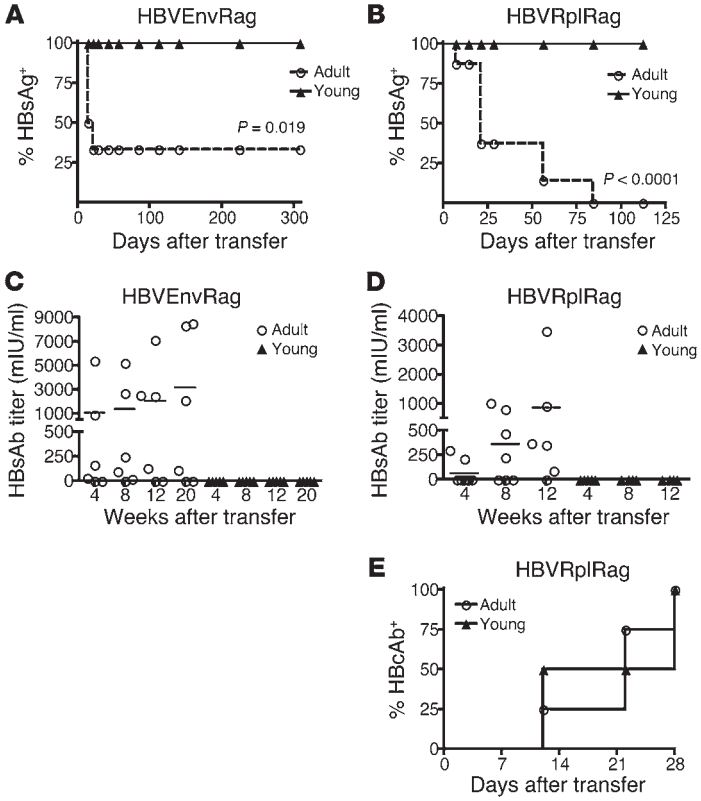

Figure 2
Transfer of adult splenocytes into young and adult HBVtgRag mice results in a difference in HBsAg clearance and HBsAb responses. Depiction of (**A** and **B**) the percentage of mice with detectable circulating HBsAg and (**C** and **D**) plasma HBsAb titer in young and adult (**A** and **C**) HBVEnvRag or (**B** and **D**) HBVRplRag mice after adoptive transfer of adult wild-type C57BL/6 mouse splenocytes. Error bars show mean ± SEM where $N \geq 5$ mice. (**E**) Presence of HBcAb in plasma of adult or young HBVRplRag mice after adoptive transfer of adult, wild-type C57BL/6 mouse splenocytes ($n = 4$ mice). Statistical significance was determined using the unpaired 2-tailed t test. Data are representative of at least 3 separate experiments.

HBV-dependent production of IL-12, IFN-γ, and IL-4 but little detectable IL-17 or IL-10 (Figure 1G). Surprisingly, ELISpot analysis of liver lymphoid cells extracted from young mice 8 days after adoptive splenocyte transfer revealed HBV-dependent cytokine production similar to that in adult mice, suggesting these young mice are initiating an immune response to the viral proteins. The liver lymphoid cells from young mice also revealed HBV-dependent production of IL-12, IFN-γ, and IL-4 and little detectable IL-17 or IL-10, although adult mice produced more IL-4 and IFN-γ (Figure 1G). We determined that cytokine production was HBV antigen-dependent by including control, *Rag1*$^{-/-}$ HBV transgene-negative C57BL/6 mice in adoptive transfer experiments (ref. 9 and Supplemental Figure 4B; supplemental material available online with this article; doi:10.1172/JCI44198DS1).

Adult HBVtgRag mice generate antibody to hepatitis B core antigen and hepatitis B surface antigen and clear hepatitis B surface antigen from circulation; young HBVtgRag mice only generate antibody to hepatitis B core antigen and do not clear hepatitis B surface antigen. When an effective immune response resulting in viral clearance is mounted in humans infected with HBV, hepatitis B surface antigen (HBsAg) disappears from the blood, as antibodies against hepatitis B core antigen (HBcAb) and HBsAg (HBsAb) are generated. In patients who become chronically infected with HBV, HBcAb is generated, but HBsAg remains detectable in the blood and HBsAb is not generated (3). Because these serum profiles of HBsAg, HBsAb, and HBcAb are signatures of viral clearance and persistence in human HBV infection, we determined the presence of these markers in the plasma of HBVtgRag mice after splenocyte transfer.

Adoptive transfer of splenocytes from adult wild-type mice into adult HBVEnvRag or HBVRplRag mice resulted in the generation of an immune response that led to life-long clearance of HBsAg from plasma, beginning 14 days after adoptive splenocyte transfer (Figure 2, A and B). In addition, these mice produced antibodies to HBsAg beginning 28 days after adoptive transfer (Figure 2, C and D), and the HBVRplRag mice produced antibodies to hepatitis B core antigen (HBcAg) beginning 12 days after adoptive transfer (Figure 2E).

However, adoptive transfer of splenocytes from adult wild-type mice into young HBVEnvRag or HBVRplRag mice resulted in failure to clear HBsAg from circulation and failure to produce HBsAb, despite their immune response to HBV (Figure 2, A–D). Notably, however, young HBVRplRag mice did generate an antibody response to HBcAg (Figure 2E).

Taken together, the effective immune responses and their kinetics observed in the adult HBVtgRag mice are comparable to those seen in adult humans experiencing acute, self-limited infection (refs. 3 and 4; Figure 3A). On the other hand, the immune responses and

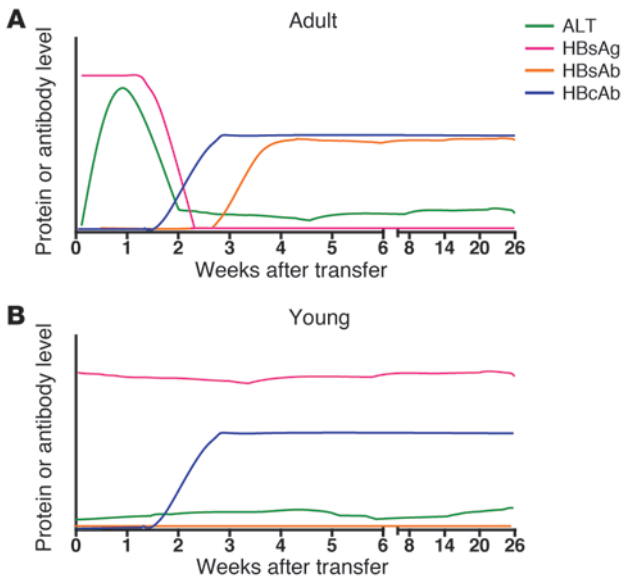

Figure 3
Patterns of serologic and molecular markers in this age-dependent model of primary HBV infection. Typical levels of ALT, HBsAg, HBsAb, and HBcAb are shown in (**A**) adult HBVtgRag mice that received adult splenocytes by adoptive transfer and (**B**) young HBVtgRag mice that received adult splenocytes by adoptive transfer. The intensity of the responses, as a function of time after infection, is indicated schematically.

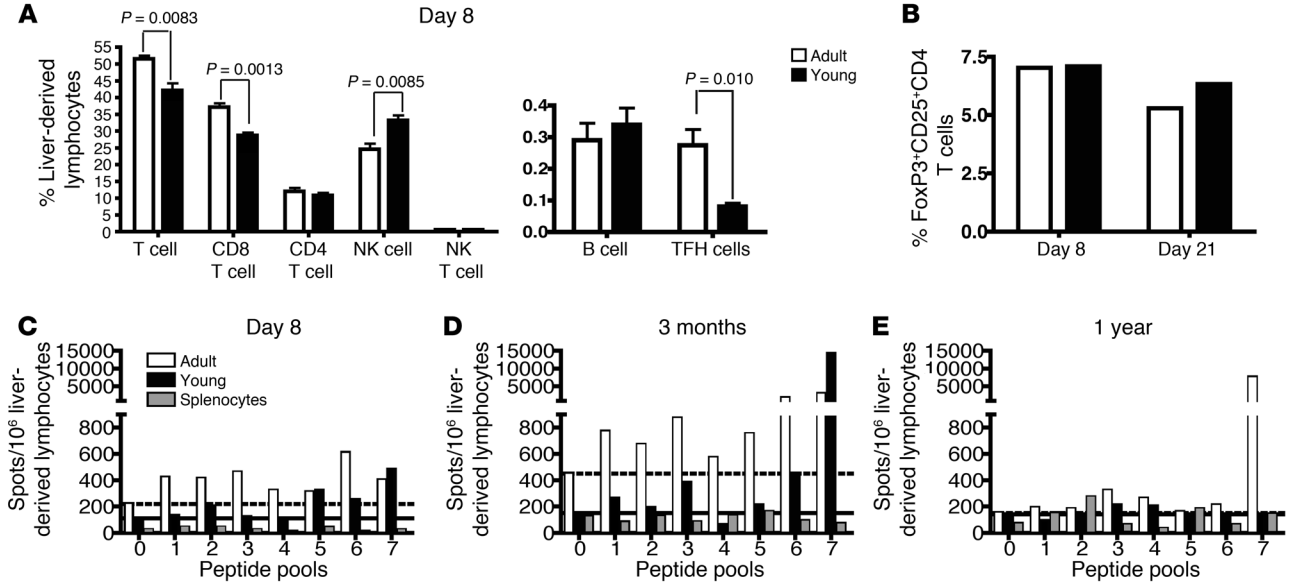

Figure 4

Adult HBVEnvRag recipient mice after adoptive transfer have more CD8+ T cells and TFH cells and elicit a more diverse and long-lived HBV-specific T cell response in the liver. (**A**) The frequency of lymphocyte populations from the livers of adult and young HBVEnvRag mice 8 days after splenocyte transfer. TFH cells are defined as CD4+, CXCR5+, ICOS+ cells. B cells are defined as CD19+, B220+ cells. Error bars depict mean ± SEM; $n = 4$ mice. Statistical significance was determined using the unpaired 2-tailed t test. (**B**) Frequency of T regulatory cells in adult and young HBVEnvRag mouse liver-derived lymphocytes on days 8 and 21 after transfer of wild-type splenocytes. Samples were pooled from $N \geq 4$ mice. Bars show percentages of CD4+-gated cells that are CD25+and FoxP3+. IFN-γ ELISpot results from young and adult HBVEnvRag mouse liver-derived lymphocytes (**C**) 8 days, (**D**) 3 months, or (**E**) 1 year after adoptive transfer. Cells were stimulated with HBV envelope peptide pools as described in Supplemental Figure 3 (pool 0 = no peptide). Dotted and solid lines indicate baseline IFN-γ levels for adult and young mice, respectively. A positive response was considered to be more than twice that of baseline. Lymphocytes were combined 1:1 with *Rag1*$^{-/-}$ splenocytes (to function as APCs); background IFN-γ levels from splenocytes are indicated by striped bars. Data are representative of at least 2 experiments; samples were pooled from $N \geq 4$ mice.

their kinetics observed in the young HBVtgRag mice are strikingly similar to those seen in young humans who develop persistent HBV infection (refs. 3 and 4; Figure 3B). Thus, this mouse model of primary HBV infection recapitulates many of the key differences in viral clearance during early life and adulthood in humans.

Analysis of young and adult HBVtgRag mice (both HBVEnvRag and HBVRplRag mice) revealed minimal differences in antigen expression in the plasma or liver. Both age groups demonstrate overlapping plasma levels and hepatocyte expression of HBsAg, demonstrating that the observed age-related differences in immune response likely do not result from differences in antigen expression (Supplemental Figure 1). Additionally, the differences in disease and antigen clearance in young and adult HBVtgRag mice is not mouse strain-specific, since these differences were also observed in HBVEnvRag mice on a B10.D2 (H-2^d) background after syngeneic splenocyte transfer (Supplemental Figure 2).

Adult HBVEnvRag recipient mice have more hepatic CD8+ T cells and T follicular helper cells. To investigate differences in the HBV-specific cellular immune responses in young and adult HBVEnvRag mice that might account for the dichotomous, age-dependent disease outcomes, we analyzed hepatic lymphocyte repertoires after adoptive transfer of adult splenocytes. We observed a significant, early increase in the percentages and absolute numbers of T cells, CD8+ T cells, and T follicular helper (TFH) cells but not of CD4+ T cells, B cells, NK, or NKT cells in the livers of adult versus young mice 8 days after adoptive transfer of splenocytes (Figure 4A and Supplemental Figure 3). There was a compensatory increase in the percentage of NK cells in the young HBVEnvRag mice, but absolute NK cell numbers were equivalent in young and adult livers (Supplemental Figure 3). Notably, there was no difference in the percentages of hepatic T regulatory cells during the critical early period after adoptive splenocyte transfer (8 days and 22 days; Figure 4B).

Adult HBVEnvRag mice elicit a more robust, diverse, and long-lived HBV-specific T cell response in the liver. It is generally accepted that the adaptive immune response to HBV is highly indicative of the course of disease. Correlative clinical studies in patients show that acute, self-limited hepatitis B is associated with a strong polyclonal and multispecific CD8+ T cell response (which can be shown in peripheral blood) early in infection. These responses involve both MHC class II–restricted CD4+ helper T cells and MHC class I–restricted CD8+ CTLs. The antiviral CTL response is directed against multiple epitopes within the HBV core, polymerase, and envelope proteins. By contrast, in chronic carriers of HBV, such initial virus-specific T cell responses are weak and exhibit narrow epitopic complexity, at least as assayed in cells from the peripheral blood (14, 15).

To examine the strength and epitopic diversity of the HBV-specific T cell response in the age-dependent mouse model of primary HBV infection, we tested liver-, spleen-, and lymph node–derived lymphoid cells in an ELISpot assay using pools of peptides, spanning the entire HBV envelope proteins (Supplemental Figure 4A). Eight days after adoptive transfer of adult splenocytes into adult HBVEnvRag mice, liver-derived T cells produced IFN-γ in response to multiple HBV envelope peptides (Figure 4C). The epitopic diversity of liver T cell responses was still seen at 3 months after adop-

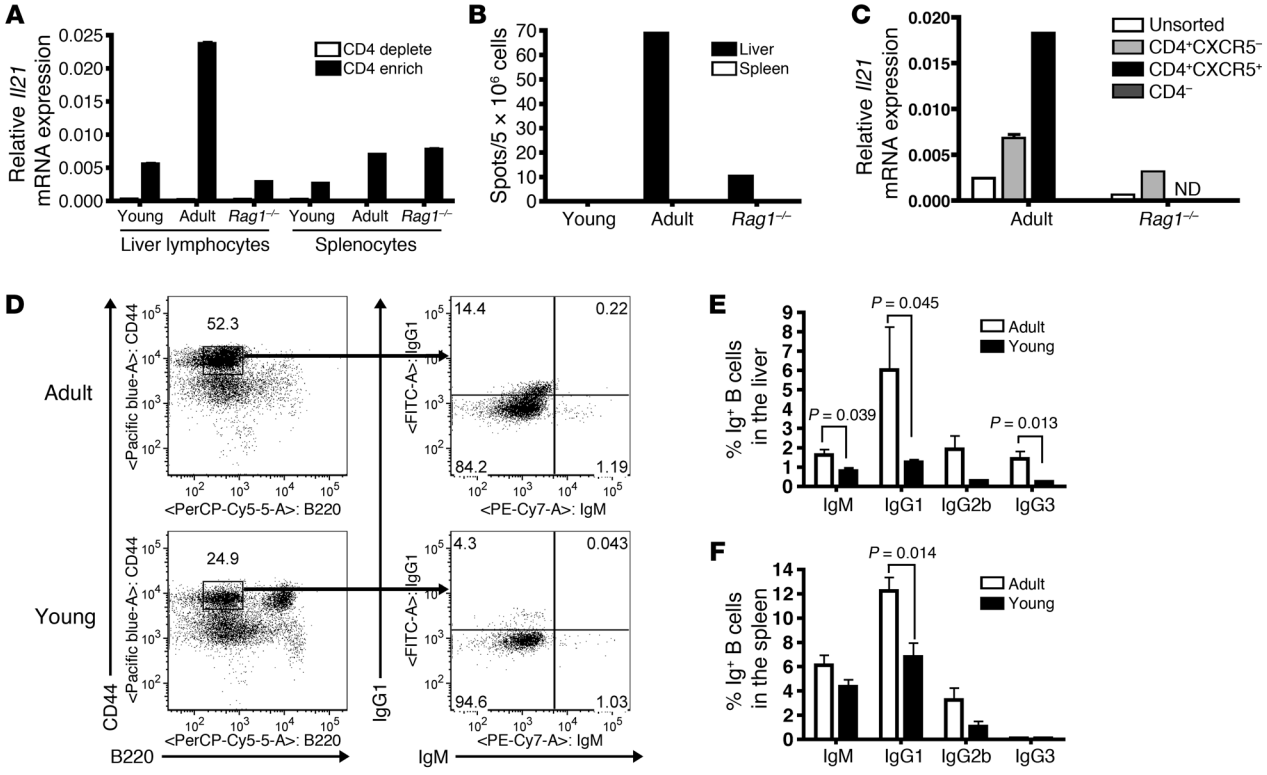

Figure 5

Liver lymphocytes from adult HBVEnvRag mice after adoptive transfer produce more IL-21 from TFH cells and have increased numbers of IgG-expressing B cells. (**A**) *Il21* mRNA levels relative to those of GAPDH in CD4+ (CD4 enrich) and CD4− (CD4 deplete) fractions from liver-derived lymphocytes or splenocytes of adult or young HBVEnvRag or adult *Rag1*$^{-/-}$ mice 8 days after adoptive transfer of splenocytes. Error bars depict duplicate wells, samples were pooled from $N \geq 6$ mice. (**B**) IL-21 protein expression determined by ELISpot on liver-derived lymphocytes and splenocytes 8 days after transfer. Samples were pooled from $N \geq 6$ mice. (**C**) *Il21* transcripts from unsorted liver lymphocytes, CXCR5−CD4+ sorted cells, CXCR5+CD4+ sorted cells (not determined for *Rag1*$^{-/-}$ due to low cell number), and CXCR5−CD4− cells from HBVEnvRag and *Rag1*$^{-/-}$ mice 8 days after transfer. Sorted cells were also CD19−DAPI−. Error bars depict triplicate wells; samples were pooled from $N \geq 4$ mice. ND, not determined. (**D**) Frequency of B cells (plasmablasts and plasma cells) in adults and young HBVEnvRag mice 3 weeks after splenocyte transfer. The left plots show B220 versus CD44 expression on TCRβ− populations, and the right plots show IgM versus IgG1 on TCRβ−, CD44hi, B220lo populations. The percentage of IgG1-, IgG2b-, IgG3-, and IgM-expressing B cells from (**E**) liver-derived lymphocytes and (**F**) splenocytes. Error bars depict mean ± SEM; $N \geq 4$ mice. Statistical significance was determined using the unpaired 2-tailed *t* test.

tive transfer (Figure 4D). After 1 year, the adult HBVEnvRag mice retained a T cell response to 2 peptide pools (Figure 4E). In young HBVEnvRag mice reconstituted with adult splenocytes, ELISpot assays also revealed the presence of HBV-specific T cell responses, which were generally weaker and less diverse than in their adult counterparts (Figure 4, C–E). Specifically, 8 days after adoptive transfer of adult splenocytes into the young HBVEnvRag transgenic mice, the liver-derived T cells contained fewer IFN-γ–producing cells and responded to fewer peptide pools, largely concentrated at the C terminus of the envelope protein (Figure 4C). In the young mice, these relatively narrow T cell responses were still present 3 months after adoptive transfer (Figure 4D), but after 1 year, no appreciable responses to the peptide pools were observed (Figure 4E). In contrast, after adoptive transfer of wild-type splenocytes, no significant IFN-γ production was observed from HBVEnvRag splenocytes or regional lymph node–derived cells or from *Rag1*$^{-/-}$ control mice in response to the peptide pools (Supplemental Figure 4, B–D).

Our antigenic peptide library consists of overlapping 15–amino acid peptides, which can be presented by both MHC class I and class II molecules. The relative contributions of CD8+ and CD4+ T cell responses were therefore investigated during the HBV-specific immune responses observed in our system. Intracellular IFN-γ staining of liver-derived lymphoid cells from the HBVEnvRag mice reconstituted with splenocytes revealed that liver-derived CD8+, CD4+, and CD4+8+ T cells all contributed to the HBV-specific T cell response (Supplemental Figure 5A).

Liver lymphocytes from adult HBVEnvRag mice after adoptive transfer produce IL-21 from TFH cells in an HBV-dependent manner and have increased numbers of IgG-expressing B cells. The blunted HBV-specific T and B cell responses in our young versus adult transgenic mice, together with the discovery that the young mice have significantly fewer TFH cells in the liver, stimulated comparative analysis of known TFH cell factors involved in the generation of antibody responses and T cell expansion. IL-21 is a type 1 cytokine, produced by TFH cells, that is critical for plasma cell generation, antibody isotype switching, and regulating immunoglobulin production and that can also promote expansion of CD8+ T cells (16–18). In models of acute and chronic infection of lymphocytic choriomeningitis virus (LCMV), IL-21 was found to be important in rescuing "exhausted" T cells after chronicity had been established, although it was not required for the specific

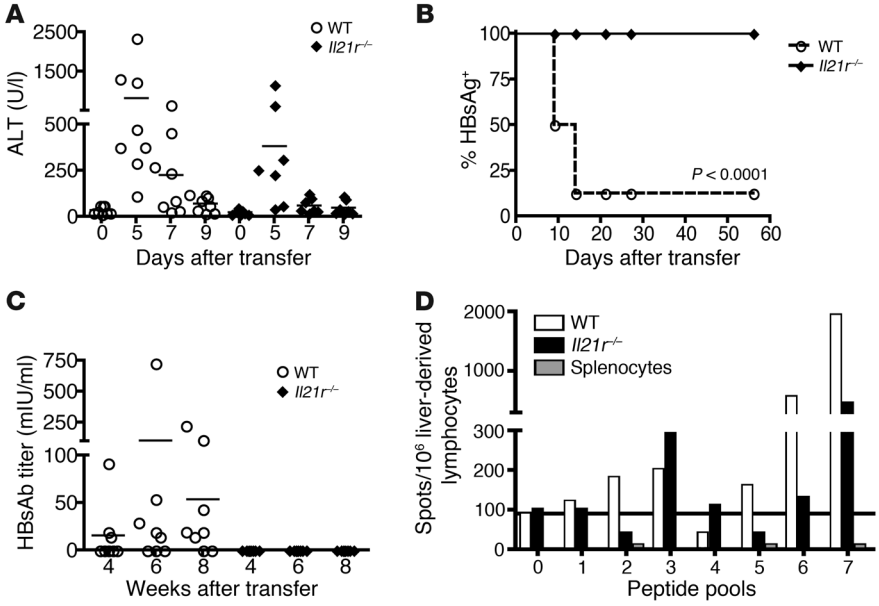

Figure 6
Adult HBVEnvRag mice fail to clear HBsAg, fail to produce HBsAb, and have a weaker and less diverse HBV-specific T cell response in the absence of IL-21R on transferred splenocytes. Adult HBVEnvRag mice were adoptively transferred with either wild-type or IL-21R–deficient C57BL/6 splenocytes. (**A**) Mice were monitored for plasma ALT (no ALT differences were observed at later time points; data not shown). Horizontal bars indicate SEM. (**B**) The percentage of mice with detectable circulating HBsAg is shown. (**C**) Mice were monitored for HBsAb titer in the plasma ($N \geq 7$ mice). Horizontal bars indicate SEM. (**D**) HBV-specific T cell responses at 2 months after transfer as measured by the IFN-γ ELISpot response of liver-derived lymphocytes stimulated with peptide pools; samples were pooled from $N \geq 4$ mice. Statistical significance was determined using the unpaired 2-tailed *t* test.

$CD8^+$ T cell response or viral control (19–21). Because these known properties of IL-21 might explain some of the immune defects in the young mice, we investigated the production and role of IL-21 in our model of HBV infection.

Eight days after adoptive splenocyte transfer, the adult HBVEnvRag mice had a 4.3-fold increase in *Il21* mRNA in liver-derived $CD4^+$ T cells (Figure 5A), as well as a substantial increase in the number of IL-21–producing, liver-derived lymphoid cells (Figure 5B), compared with that in the young HBVEnvRag mice. The HBV-dependent increase in *Il21* mRNA occurred mostly in the $CD4^+$ T cell subset that expressed the chemokine receptor, CXCR5 (78% of these $CXCR5^+CD4^+$ T cells were $ICOS^+$; Figure 5C). Thus, the majority of IL-21–producing cells were TFH cells. In contrast, we did not detect an increase in HBV-dependent *Il21* transcripts or production of IL-21 protein in the spleen (Figure 5, A and B).

Analysis of immunoglobulin expression on plasma cells and plasmablasts in the liver and spleen of adult and young HBVEnvRag mice 3 weeks after adoptive splenocyte transfer revealed that the adult mice exhibited a significant increase in the number of plasma cells and plasmablasts that were differentiated into IgG1-, IgG2b-, and IgG3-expressing cells (Figure 5, D–F). This B cell differentiation and class-switch difference occurred to a lesser extent in the spleen than in the liver (Figure 5, E and F).

IL-21 receptor on transferred splenocytes is necessary to generate an immune response that correlates with viral clearance. To test whether an IL-21–dependent immune response is necessary to generate the HBV antigen clearance seen in adult HBVEnvRag mice, we used splenocytes from IL-21 receptor–deficient (IL-21R–deficient) mice as donor cells in adoptive transfer experiments (17). These experiments showed that lack of IL-21R on adoptively transferred splenocytes resulted in immune responses in adult HBVEnvRag mice that resembled the responses in young HBVEnvRag mice and resulted in HBV antigen persistence. More specifically, lack of IL-21R on donor splenocytes prevented hepatitis (ALT elevation) during the peak of the adaptive immune response (day 7) but did not appear to influence hepatitis during the "NKT cell phase" of disease (refs. 9 and 10; Figure 6A). Furthermore, lack of IL-21R on donor splenocytes resulted in the absence of clearance of circulating HBsAg (Figure 6B) and the absence of HBsAb production (Figure 6C). Finally, ELISpot analysis using the pools of HBV envelope peptides demonstrated that the absence of IL-21R on donor splenocytes caused a weaker and less diverse T cell response to HBV envelope peptides 8 weeks after adoptive transfer (Figure 6D). Intracellular IFN-γ staining of liver-derived lymphoid cells from HBVEnvRag mice 2 months after adoptive transfer of wild-type or IL-21R–deficient splenocytes revealed that lack of IL-21R on donor cells resulted in a greater reduction in the strength and diversity of the $CD8^+$ T cell response than of the $CD4^+$ T cell response (Supplemental Figure 5).

Increased IL-21 expression is part of an effective immune response to HBV in adults acutely infected with HBV who clear the virus. The mouse model and the data presented thus far led us to hypothesize that increased IL-21 expression is a key part of a primary immune response to HBV that results in viral clearance and immunity in adults and that increased IL-21 expression would not occur in a primary immune response to HBV in newborn or young individuals who do not clear the virus. Although it is not ethical to obtain blood or liver tissue from newborns or young children acutely infected with HBV, we can obtain blood from adults acutely infected with HBV with evidence of hepatitis as well as from patients chronically infected with HBV (who were likely infected young), during a hepatitic flare of chronic infection. Both groups typically have similar and overlapping plasma viral titers and ALT elevation.

We therefore tested this hypothesis by isolating RNA from PBMCs from adult patients acutely infected with HBV and hepatitis, adult patients chronically infected with HBV during a hepatitic flare, adult patients chronically infected with HBV without active hepatitis, and uninfected adult individuals. Strikingly, there was a significant 7-fold increase in relative expression of *IL21* mRNA in PBMCs from patients acutely infected with HBV who cleared the virus as compared with PBMCs from patients chronically infected with HBV who have hepatitic flares but fail to clear the virus (Figure 7). Notably, we also did not observe increased *IL21* mRNA in healthy individuals or in inactive chronic carriers (low ALT and low

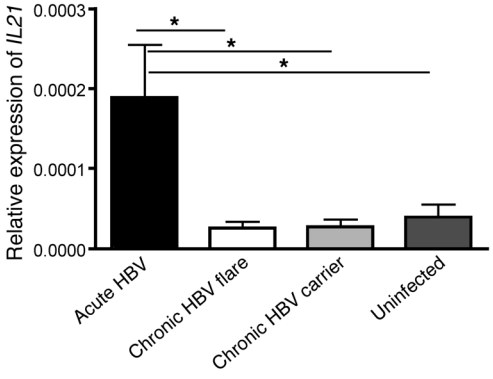

Figure 7

Patients acutely infected with HBV express more *IL21* mRNA in their PBMCs compared with patients with chronic HBV infection during actively flaring disease, inactive chronic HBV carriers, and healthy individuals. *IL21* mRNA relative to that of GAPDH in PBMCs taken from patients with acute HBV infection (high viral load, high ALT, IgM core Ab^+, $HBsAg^+$, and clinical history of exposure); patients with chronic HBV infection with a flare of disease (high ALT, high viral load, $HBsAg^+$, and known history of chronic infection); patients with chronic HBV infection (low ALT, low viral load, and $HBsAg^+$); and healthy, uninfected patients (low ALT and $HBsAg^-$) is shown. Error bars depict mean ± SEM; $N \geq 5$. Statistical significance was determined using the ANOVA with Tukey's post-hoc test. $^*P < 0.05$.

or undetectable viral load; Figure 7). Since all the studied patients with acute hepatitis B (5 patients) cleared the virus (>90% of adults clear), we have not yet been able to study adult patients who fail to clear. This will be a primary objective of future human studies.

Discussion

Herein, we describe a model of age-dependent HBV infection that suggests that the age of the hepatic immune-priming environment in HBVtgRag mice significantly influences the immune responses that result in viral clearance or persistence. Young mice reconstituted with an adult immune system generated an immune response with a serological profile ($HBcAb^+$, $HBsAb^-$, $HBsAg^+$) that mirrors viral persistence in young humans. Furthermore, young mice that received adult splenocytes exhibited a weaker and less diverse HBV-specific T cell response, analogous to the immune responses seen in the peripheral blood of patients who develop chronic HBV infection.

As with all animal models of human disease, certain aspects of natural HBV infection are not captured. For example, the mice are not naturally infected by HBV but are producing transgenic HBV proteins and virions. Also, in the HBV transgenic model, a naive immune system abruptly encounters hepatocytes expressing high levels of HBV antigen or virions. Whether kinetic differences in HBV infection and replication also influence the evolution of the immune response, as suggested by a different animal model (22), remains to be determined.

Our data in the mouse model demonstrate that the young HBV transgenic mice generated an immune response to HBV. Specifically, the young mice exhibited HBV-dependent liver inflammation; produced HBV-driven IL-4, IL-12, and IFN-γ; and generated a T cell response to HBV envelope peptides. In addition, the young mice (like human babies) generated an antibody response to HBcAg. Furthermore, the immune system of 3- to 4-week-old mice has developed beyond the typical window of neonatal T cell tolerance induction (23), and we demonstrated that 3- to 4-week-old C57BL/6 mice, analogous to young humans, can mount robust antibody responses to HBsAg when vaccinated at peripheral sites with the recombinant HBV vaccine (Supplemental Figure 6).

The differences in immune responses and mechanisms we observed in the young mice, as compared with those in adult mice, include an inability to generate an HBsAb response, fewer $CD8^+$ T cells in the liver, an inability to diversify and sustain strong HBV-specific T cell responses, a paucity of IL-21–producing TFH cells in the liver, and fewer IgG-expressing B cells in the liver. In these young mice, we did not observe global B cell nonresponsiveness to HBV antigens, global T cell nonresponsiveness to HBV antigens, differences in the absolute number or proportion of T regulatory cells in the liver on days 8 and 22 after adoptive transfer, or differences in production of IL-10 in the liver.

Taken together, these data suggest that mechanisms other than those classically perceived as those of "immune tolerance" are involved in the selective lack of immune responses in young mice. Future studies are needed to address whether classical mechanisms of immune tolerance accompany or follow the mechanisms we observe in young mice and contribute to the selective differences in immune responses that occur in young mice and also in humans infected when they are young.

Using this model, we have identified a potentially key role in the liver for IL-21 in determining the effectiveness of the primary antiviral immune response to HBV and, ultimately, the long-term immune response to this virus. Our data suggest a model whereby the young have ineffective hepatic TFH cell priming and/or trafficking, leading to decreased IL-21 production at sites at which it is essential for optimal generation of specific $CD8^+$ T and B cell responses that are crucial for clearance of viral antigens. Indeed, IL-21R deficiency results in viral persistence. These data expand the recognized role of IL-21 in viral infection. Previous studies using LCMV infection (19–21) had demonstrated that IL-21 deficiency exacerbated immune exhaustion after infection with the chronic clone 13 strain of LCMV, but they did not identify a role for IL-21 in converting a self-limited infection with the Armstrong strain of LCMV to chronic infection (19–21). Additionally, our data support and expand observations in a chimpanzee model of acute HBV infection that $CD4^+$ T cells are important for viral clearance. In that model, early activation of $CD4^+$ T cells correlates with an influx of HBV-specific CD8 T cells into the liver, and animals depleted of $CD4^+$ cells become persistently infected when inoculated with a dose of HBV that is typically cleared (24). Our data support a pivotal role of $CD4^+$ T cells in effecting viral clearance and indicate that a specific subset of $CD4^+$ T cells, the TFH cells, is critical in determining immune responses to the virus and disease outcome. Furthermore, our correlative data suggest a role for IL-21 and TFH cells in facilitating an effective immune response in humans acutely infected with HBV. Adult patients have increased IL-21 expression during the primary immune response to HBV that results in viral clearance and immunity, but this does not occur in chronically infected patients during a hepatitic flare. Thus, our findings in the mouse model may predict aspects of the human disease. Finally, our demonstration that the defect in HBV-dependent IL-21 production and the HBV-specific adaptive immune response is liver centered suggests that physiologically important hepatic immune priming may be required for natural HBV immunity in humans.

In sum, our model of HBV clearance and persistence mimics several aspects of the age-related dichotomy in human HBV

infection outcome, and we propose what we believe to be a new hypothesis to explain the dichotomous, age-dependent outcome of HBV infection in humans. This model provides a rational experimental system to further dissect the immune responses that lead to viral persistence or clearance and to examine the reversibility of the altered immune priming that facilitates HBV persistence. The fact that a minority of humans chronically infected with HBV since childhood can generate HBsAb and clear viral antigens either spontaneously or after therapeutic interventions, such as IFN-α or nucleoside/nucleotide analogs, strongly suggests that repriming of an ineffective immune response can be achieved. Our model opens the door for rational design of new therapeutic interventions and provides clearly defined experimental outcomes as a framework for testing therapeutic candidates. The development of new HBV therapeutic strategies that effectively tilt immune responses either toward viral clearance or away from immune-mediated liver injury should provide novel and much needed therapeutic interventions for this globally important disease.

Methods

Mice and experimental system. C57BL/6 wild-type mice were purchased from The Jackson Laboratory. IL-21R–deficient mice were provided by Warren Leonard (17). HBVtgRag1 mice used were previously described (9). Briefly, HBVEnvRag mice were generated using HBVEnv$^+$ mice (lineage 107-5D; gift from F. Chisari, The Scripps Research Institute, La Jolla, California, USA; ref. 11) backcrossed to *Rag1*$^{-/-}$ C57BL/6 mice for 15 generations. HBVEnvRag mice contain the entire envelope (subtype ayw) protein-coding region under the constitutive transcriptional control of the mouse albumin promoter. HBVRplRag mice were generated using HBVRpl mice (lineage 1.3.46; gift from F. Chisari; ref. 12) crossed to *Rag1*$^{-/-}$ C57BL/6 mice for 15 generations. HBVRplRag mice contain a terminal redundant HBV DNA construct and produce infectious virus in their hepatocytes and in the proximal convoluted tubules of their kidneys.

Young (3- to 4-week-old, preweaned) or adult (8- to 12-week-old) HBVtgRag mice were given 10^8 syngeneic splenocytes from wild-type or mutant mouse strains via tail vein injection. Young mice were weaned at the date of transfer. Mice were followed for alanine aminotransferase by using an ALT-L3K Kit (Diagnostic Chemicals Limited) on a Cobas Miras Plus analyzer (Roche Diagnostics). Mice were kept in microisolater cages in a specific pathogen–free facility, and the UCSF Institutional Animal Care and Use Committee approved all animal experiments done in this study.

HBV protein assays. Plasma was collected and assayed for the presence of HBsAg by using ETI-MAK 2Plus (DiaSorin). HBsAb was quantified by using ETI-AB-AUK PLUS and ABAU standard set (DiaSorin). This kit detects all isotypes of HBsAb and has a sensitivity of 5 milli-IU (mIU/ml). Plasma from transfer HBVRplRag mice was assayed for presence of HBcAb by using ETI-AB-COREK PLUS (DiaSorin). All assays were read on ELx800 (Biotek Instruments Inc.) at wavelengths of 450 nm and 630 nm.

Lymphocyte isolation. Lymphocytes were isolated from the liver after perfusion and digestion. Briefly, mice were perfused via the inferior vena cava, using digestion media (RPMI-1640 containing 5% FBS, 0.2 mg/ml crude collagenase [Crescent Chemical], and 0.02 mg/ml DNase I [Roche Diagnostics]). Livers were forced through a 70-μM filter using a syringe plunger, and debris was removed by centrifugation (30 *g* for 3 minutes). Supernatants were collected and spun for 10 minutes at 650 *g*. Lymphocytes were isolated using a 60/40 Percoll gradient. Lymphocytes from spleen and lymph node were isolated using standard methods.

ELISpot. IFN-γ, IL-4 (BD Biosciences), IL-12, IL-10, IL-17 (R&D Systems), and IL-21 ELISpot assays were performed on unstimulated liver lymphocytes. Peptide pool ELISpot assays were performed by using IFN-γ ELISpot assays plated with lymphocytes from transferred animals combined 1:1 with *Rag1*$^{-/-}$ splenocytes to provide optimal APC stimulation. Fifteen-mer peptides were generated across the whole envelope protein in 11–amino acid overlaps (Sigma-Aldrich). Pools included 11–14 peptides (Supplemental Figure 3). Cells were incubated with peptides at a final concentration of 5 μg/ml for each peptide. IL-21 ELISpot assays were performed using MultiScreen IP plates (Millipore) coated overnight with anti-mouse IL-21 antibody (5 μg/ml; R&D Systems). Lymphocytes were plated for 24 hours before secondary incubation with biotinylated anti-mouse IL-21 antibody (2 μg/ml; R&D Systems) followed by streptavidin-HRP (BD Biosciences) and developed using AEC substrate (BD Biosciences).

Cell sorting. Liver-derived lymphocytes and splenocytes were prepared as described above. Cells were blocked and stained with anti–CD4-coated Microbeads (L3T4; Miltenyi Biotec). CD4$^+$ fractions showed 79%–82% purity, and CD4$^-$ fractions showed less than 2% CD4$^+$ cells present. Separately, liver lymphocytes were stained with Pacific Blue–conjugated anti-CD4, biotinylated anti-CXCR5, and FITC-conjugated anti-CD19 as described below, followed by PE-conjugated streptavidin. The CD19$^-$DAPI$^-$ gated population was sorted for CD4$^+$CXCR5$^-$, CD4$^+$CXCR5$^+$, and double-negative populations by using MoFlo flow cytometer (Beckman Coulter).

Histology. Liver tissue was fixed in 4% PFA or placed in 10% formalin and embedded in paraffin blocks. Five-micron slices were cut. PFA-fixed tissues were stained with goat polyclonal anti-HBsAg (Abcam ab17183) by the Microscopy and Advanced Imaging Core Facility at the San Francisco VA Medical Center. Formalin-fixed tissues were stained with H&E according to standard protocols.

Flow cytometry. Lymphocytes were prepared as above. Cells were stained according to standard protocols with combinations of the following anti-mouse antibodies: APCCy7-conjugated anti-CD4 (clone GK1.5), APC-conjugated anti-TCRβ or biotinylated anti-TCRβ (clone H57-597), PerCPCy5.5-conjugated anti-NK1.1 (clone PK136), Pacific Blue–conjugated anti-CD8 (clone 53-6.7), biotinylated anti-CXCR5 (clone 2G8), PerCPCy5.5-conjugated anti-B220 (clone RA3-6B2), and FITC-conjugated anti-FAS (all from BD Biosciences) and PE-conjugated anti-ICOS (clone 7E.17G9), Pacific Blue–conjugated anti-CD19 (clone 57-0193), biotinylated anti-GL7, and efluor450-conjugated anti-CD44 (clone IM7) (all from eBioscience). When applicable, cells were stained with QDot 605–conjugated streptavidin (Invitrogen). Cells were analyzed using an LSRII flow cytometer (Becton Dickinson) and FlowJo software (Tree Star).

T regulatory cells were identified by using the mouse regulatory T cell staining kit (eBioscience). For B cell isotype switch experiments, cells were stained to detect CD19, B220, CD44, and TCRβ as described above. Following surface staining, cells were fixed and permeabilized using Cytofix/Perm (BD Biosciences) and stained with PE-conjugated anti-CD138 (clone 281-2; BD Biosciences) for 40 minutes at 4°C. Cells were washed and stained overnight at 4°C with PECy7-conjugated anti-IgM (clone 11/14; eBioscience), along with FITC-conjugated anti-IgG1 (clone SB77e; Southern Biotech), FITC-conjugated anti-IgG2b (clone R12-3; BD Biosciences), or FITC-conjugated anti-IgG3 (clone R40-82; BD Biosciences) or appropriate isotype-matched control immunoglobulin. Intracellular cytokine was detected using standard procedure. Peptide pools were used to stimulate T cells at a final concentration of 10 μg/ml. Cells were stained for cell surface with CD8, CD4, and TCRβ and intracellularly for IFN-γ.

RNA extraction and real-time PCR. RNA isolated from lymphocytes was prepared by using an RNeasy Micro Kit (Qiagen) using a blunt syringe disruption. One μg or 0.14 μg isolated RNA was reverse transcribed using the iScript cDNA synthesis kit (Bio-Rad). Real-time PCR was performed on 2.5 μl cDNA product using iTaq SYBR Green Supermix with ROX (Bio-Rad) and the following primers: GAPDH forward, 5′-GGAGCGAGACCCCACTAACA-3′; GAPDH reverse, 5′-ACATACTCAGCACCGGCCTC-3′ (25);

IL-21 forward, 5′-TCATCATTGACCTCGTGGCCC-3′; IL-21 reverse, 5′-ATCGTACTTCTCCACTTGCAATCC-3′ (26); IFN-γ forward, 5′-CAGGAAGCGGAAAAGGAGTCG-3′; IFN-γ reverse, 5′-GTCACTGCAGCTCTGAATGTT-3′ (gift from Lee Reinhardt and Richard Locksley, both from UCSF); IL-17A forward, 5′-GCTCCAGAAGGCCCTCAG-3′; and IL-17A reverse, 5′-CTTTCCCTCCGCATTGAC-3′. Real-time PCR was performed on the 7300 Real Time PCR System (Applied Biosystems).

Patient samples and IL-21 RNA expression. Five patients with confirmed acute HBV infection, 6 patients with confirmed inactive chronic HBV infection, 5 patients with confirmed chronic HBV infection exhibiting a flare of disease, and 6 healthy volunteers were enrolled at California Pacific Medical Center, Department of Liver Disease Management and Transplant, Hepatology Research Center, San Francisco, California, USA. The study was approved by the California Pacific Medical Center Institutional Review Board. All subjects reviewed and signed human research informed consent forms. Blood samples were drawn by a licensed phlebotomist along with clinical serology samples. Serology, serum HBV DNA, and ALT data was obtained from the patients' clinical medical records with their permission. Acutely infected HBV patients had confirmed high viral loads ($2.44 \times 10^7 \pm 2.43 \times 10^7$ IU/ml); elevated ALT (922–2,400 U/l), $HBsAg^+$, and IgM core Ab^+; and a clinical history of exposure. Inactive chronic HBV carriers had confirmed low viral loads ($1.24 \times 10^3 \pm 5.6 \times 10^2$ IU/ml) and low ALT (20–29 U/l) and $HBsAg^+$. Chronic HBV patients exhibiting a flare in disease had confirmed high viral loads ($3.05 \times 10^8 \pm 3.04 \times 10^8$ IU/ml), elevated ALT (92–1,090 U/l) and $HBsAg^+$, and known history of chronic infection. Uninfected controls had confirmed low ALT (16–32 U/l) and $HBsAg^-$.

RT-PCR assays were performed on previously frozen PBMCs that were isolated by a Ficoll gradient centrifugation. RNA was isolated from $1–2 \times 10^6$ live human PBMCs using an RNeasy Micro Kit (Qiagen) with QIAshredder disruption, and 0.25 μg isolated RNA was reverse transcribed using the iScript cDNA synthesis kit (Bio-Rad). Real-time PCR was performed on 2.5 μl cDNA product using iTaq SYBR Green Supermix with ROX (Bio-Rad) and the following primers: GAPDH forward, 5′-TGATGACATCAAGAAGGTGG-3′; GAPDH reverse, 5′-TTTCTTACTCCTTGGAGGCC-3′; IL-21 forward, 5′-GCAGGGAGAAGACAGAAACA-3′; and IL-21 reverse, 5′-GGAATCTTCACTTCCGTGTG-3′ (Real Time Primers LLC).

Statistics. Statistics were performed using Prism software (GraphPad Software). Statistical significance was determined using the 2-tailed unpaired Student's *t* test when 2 groups were compared. Statistical significance was determined using 1-way ANOVA Tukey's multiple comparison test when more than 2 groups were compared. A *P* value less than 0.05 was considered significant. *P* values for individual data sets are stated in the figure or in the legends.

Acknowledgments

We would like to thank Anna Bogdanova, Christine Van Horn, and Gerald Willkom for technical support and mouse colony management. We would also like to acknowledge Kahee Jo and Arthur Rayz for their thankless volunteer work in the laboratory. We graciously thank Mark Ansel, Jason Cyster, Don Ganem, Mehrdad Matloubian, and Peggy Weintrub for advice and Samuel Baron, Lewis Lanier, Marion Peters, and Jay Ryan for advice and critical comments on the manuscript. We would also like to thank Lee Reinhardt, João Pereira, Courtney Crane, and Ann Erickson for technical advice. Lastly, we would like to thank the patients and healthy volunteers for their blood donation used in this study. This work was supported by NIH NIAID (RO1AI068090), UCSF Liver Center (P30DK026743), Cancer Research Institute, Burroughs Wellcome Fund, and Ibrahim El-Hefni Technical Training Foundation. Throughout this work, J. Publicover was supported by National Research Service Award Hepatology Training grant (T32DK060414) and A.P. Gianinni Foundation. W.J. Leonard and R. Spolski were supported by the Division of Intramural Research, National Heart, Lung, and Blood Institute.

Received for publication November 18, 2010, and accepted in revised form December 22, 2010.

Address correspondence to: Jody Baron, 513 Parnassus Ave., S-357C, Box 0538, San Francisco, California 94158, USA. Phone: 415.476.5728; Fax: 415.476.0659; E-mail: jody.baron@ucsf.edu.

Silvia Vilarinho's present address is: Department of Medicine, Yale University School of Medicine, New Haven, Connecticut, USA.

1. Lee WM. Hepatitis B virus infection. *N Engl J Med*. 1997;337(24):1733–1745.
2. Robinson WS. Hepatitis B virus and hepatitis D virus. In: Mandell GL, Bennett JE, Dolin R, eds. *Principles and Practice of Infectious Diseases*. 4th ed. New York, New York, USA: Churchill Livingstone; 1995:1406–1439.
3. Ganem D, Prince AM. Hepatitis B virus infection--natural history and clinical consequences. *N Engl J Med*. 2004;350(11):1118–1129.
4. Liang TJ. Hepatitis B: the virus and disease. *Hepatology*. 2009;49(5 suppl):S13–S21.
5. Chisari FV, Isogawa M, Wieland SF. Pathogenesis of hepatitis B virus infection. *Pathol Biol (Paris)*. 2010; 58(4):258–266.
6. Milich DR, Jones J, Hughes J, Maruyama T. Role of T-cell tolerance in the persistence of hepatitis B virus infection. *J Immunother Emphasis Tumor Immunol*. 1993;14(3):226–233.
7. Milich DR, Jones JE, Hughes JL, Price J, Raney AK, McLachlan A. Is a function of the secreted hepatitis B e antigen to induce immunologic tolerance in utero? *Proc Natl Acad Sci U S A*. 1990;87(17):6599–6603.
8. Pungpapong S, Kim WR, Poterucha JJ. Natural history of hepatitis B virus infection: an update for clinicians. *Mayo Clin Proc*. 2007;82(8):967–975.
9. Baron JL, Gardiner L, Nishimura S, Shinkai K, Locksley R, Ganem D. Activation of a nonclassical NKT cell subset in a transgenic mouse model of hepatitis B virus infection. *Immunity*. 2002;16(4):583–594.
10. Vilarinho S, Ogasawara K, Nishimura S, Lanier LL, Baron JL. Blockade of NKG2D on NKT cells prevents hepatitis and the acute immune response to hepatitis B virus. *Proc Natl Acad Sci U S A*. 2007; 104(46):18187–18192.
11. Chisari FV, et al. Expression of hepatitis B virus large envelope polypeptide inhibits hepatitis B surface antigen secretion in transgenic mice. *J Virol*. 1986;60(3):880–887.
12. Guidotti LG, Matzke B, Schaller H, Chisari FV. High-level hepatitis B virus replication in transgenic mice. *J Virol*. 1995;69(10):6158–6169.
13. Mombaerts P, Iacomini J, Johnson RS, Herrup K, Tonegawa S, Papaioannou VE. RAG-1-deficient mice have no mature B and T lymphocytes. *Cell*. 1992; 68(5):869–877.
14. Baumert TF, Thimme R, von Weizsacker F. Pathogenesis of hepatitis B virus infection. *World J Gastroenterol*. 2007;13(1):82–90.
15. Chisari FV, Ferrari C. Hepatitis B virus immunopathogenesis. *Annu Rev Immunol*. 1995;13:29–60.
16. Ozaki K, et al. Regulation of B cell differentiation and plasma cell generation by IL-21, a novel inducer of Blimp-1 and Bcl-6. *J Immunol*. 2004; 173(9):5361–5371.
17. Ozaki K, et al. A critical role for IL-21 in regulating immunoglobulin production. *Science*. 2002; 298(5598):1630–1634.
18. Spolski R, Leonard WJ. IL-21 and T follicular helper cells. *Int Immunol*. 2010;22(1):7–12.
19. Elsaesser H, Sauer K, Brooks DG. IL-21 is required to control chronic viral infection. *Science*. 2009; 324(5934):1569–1572.
20. Frohlich A, et al. IL-21R on T cells is critical for sustained functionality and control of chronic viral infection. *Science*. 2009;324(5934):1576–1580.
21. Yi JS, Du M, Zajac AJ. A vital role for interleukin-21 in the control of a chronic viral infection. *Science*. 2009;324(5934):1572–1576.
22. Wieland S, Thimme R, Purcell RH, Chisari FV. Genomic analysis of the host response to hepatitis B virus infection. *Proc Natl Acad Sci U S A*. 2004; 101(17):6669–6674.
23. Guerau-de-Arellano M, Martinic M, Benoist C, Mathis D. Neonatal tolerance revisited: a perinatal window for Aire control of autoimmunity. *J Exp Med*. 2009;206(6):1245–1252.
24. Asabe S, et al. The size of the viral inoculum contributes to the outcome of hepatitis B virus infection. *J Virol*. 2009;83(19):9652–9662.
25. Wiwi CA, Gupte M, Waxman DJ. Sexually dimorphic P450 gene expression in liver-specific hepatocyte nuclear factor 4alpha-deficient mice. *Mol Endocrinol*. 2004;18(8):1975–1987.
26. Nurieva R, et al. Essential autocrine regulation by IL-21 in the generation of inflammatory T cells. *Nature*. 2007;448(7152):480–483.